# Experimental methods in X-ray crystallography

4

HUGO L. MONACO

## Introduction

This chapter discusses the experimental methods used to study the diffraction of X-rays by crystalline materials. Although, as seen in Appendix 3.B (pp. 195 and 198), electrons and neutrons are also diffracted by crystals, we will concentrate our attention on X-ray diffraction. We begin discussing how X-rays are produced and how one can define the beam of radiation that will interact with the crystalline sample. The specimens that will receive our attention are single crystals and polycrystalline materials, that is aggregates of a very large number of very small crystals. We discuss the methods used to record the diffraction pattern and to measure the intensities of the X-rays scattered by these two types of specimen in separate sections. The ultimate goal of extracting structure factor amplitudes from diffracted intensities requires the application of a series of correction factors. This process, called data reduction, is discussed in the final section of the chapter.

## X-ray sources

### Conventional generators

All the standard laboratory sources normally used for X-ray diffraction experiments generate radiation using the same physical principles but can vary substantially in their construction details. The two types of conventional generators that are used in conjunction with the data recording devices discussed on pp. 245 and 287 are sealed-tube and rotating-anode generators. Most of the techniques used for diffraction data collection require monochromatic radiation. Due to the way in which radiation is produced in the conventional generators, only a discrete number of possible wavelengths can be selected for experimental use. This limited choice and the difference in intensity are two of the major differences between this type of radiation and that generated by synchrotrons.

### The origin of X-rays in the conventional sources

X-rays are produced when a beam of electrons, accelerated by a high voltage, strikes a metal target and is therefore rapidly decelerated by collision with the metal atoms. Most of the electrons do not lose their

energy in a single collision but do it gradually through multiple events. The result is the production of a continuous spectrum of X-rays called white radiation. If all of the energy carried by an electron is transformed into radiation, the energy of an X-ray photon is

$$E_{max} = h\nu_{max} = eV$$

where $h$ is Planck's constant, $\nu_{max}$ the photon frequency and the subscript max indicates that this is the maximum possible energy, $e$ is the charge of the electron, and $V$ the accelerating potential.

If we substitute the frequency in terms of the wavelength

$$h\nu_{max} = hc/\lambda_{min} = eV$$

and

$$\lambda_{min} = hc/eV = 12\,398/V \tag{4.1}$$

where the potential $V$ has to be measured in volts and the minimum wavelength is obtained in angstroms. This equation shows that there is a minimum value for the wavelength of the X-rays that can be obtained by this process which is a function of the voltage accelerating the electrons.

Total conversion of the electron energy into radiation is not a highly probable event and therefore the radiation of the highest intensity is obtained at a somewhat longer wavelength. Figure 4.1 shows some continuous X-ray spectra as a function of the accelerating voltage. Notice that as the voltage is increased both the minimum wavelength and the position of the intensity maximum shift to the left. The intensity maximum is found at a wavelength which is approximately 1.5 times $\lambda_{min}$.

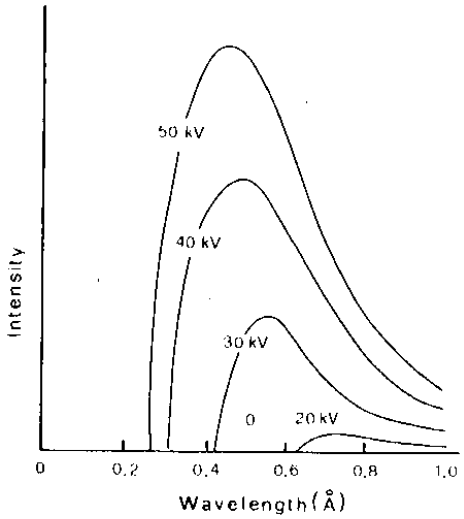


**Fig. 4.1.** X-ray white radiation spectra as a function of the accelerating voltage.

The total X-ray intensity generated per second in this way, a quantity which is proportional to the areas under the curves, can be calculated using the equation

$$I_w = AiZV^n \tag{4.2}$$

where $A$ is a proportionality constant, $i$ the electrical current, a measure of the number of electrons which are generating X-rays, $Z$ is the atomic number of the target, $V$ the accelerating potential, and $n$ a constant with a value of about 2.

When the energy of the electrons striking the target is higher than a certain threshold value, a second type of spectrum, discontinuous and with very sharp lines, appears superimposed on the white radiation curves just described. This second spectrum is called the characteristic spectrum because its peaks are found at precisely defined wavelengths which depend on the material constituting the target. The characteristic spectrum of copper is shown in Fig. 4.2. The electrons with an energy above the threshold potential are capable of ionizing the target atoms by ejecting an electron from one of the inner shells. When that happens another electron from a higher atomic energy level can move in to fill the vacancy created and, since the new level has a lower energy, emit the energy difference as a characteristic X-ray photon whose wavelength depends on the difference in energy between the two levels involved.

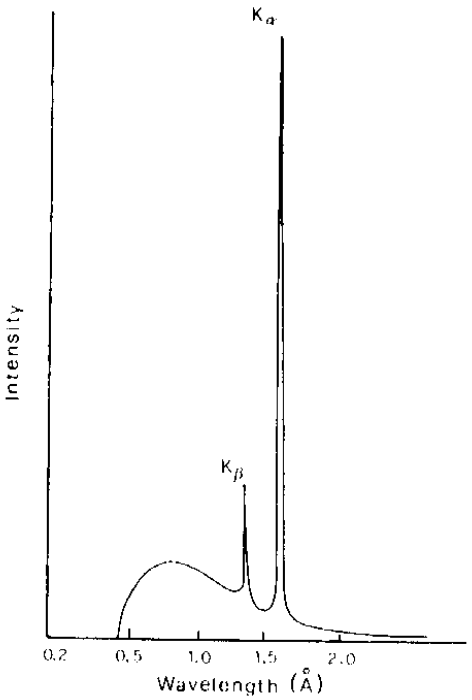


**Fig. 4.2.** Characteristic spectrum of copper superimposed on the white radiation spectrum. Notice the ratio of the relative intensities of the $K_\alpha$ and $K_\beta$ lines.

The characteristic lines of this type of spectrum are called K, L, and M and correspond to transitions from higher energy orbitals to the K, L, and M orbitals, that is to the orbitals of principal quantum numbers $n = 1$, 2,

and 3. When the two orbitals involved in the transition are adjacent the line is called $\alpha$, if they are separated by another shell, the line is called $\beta$. Thus, the Cu $K_\alpha$ line is produced by a copper target in which the atoms lost an electron in the orbital of $n = 1$ and the vacancy was filled by an electron of the orbital $n = 2$. The X-ray photon energy is the difference between these two energy levels. Since for every principal quantum number $n$ there are $n$ energy levels corresponding to the possible values of the quantum number 1 (from 0 to $n - 1$), the $\alpha$ and $\beta$ lines are actually split into multiple lines that are very close to one another because the difference between these energy levels is small. Still, X-ray radiation corresponding to all the possible energy differences is not observed because some energy transitions are forbidden by the selection rules. Thus, although Fig. 4.2 has a scale on the abscissa which cannot show it, the Cu $K_\alpha$ line is actually split into a doublet, the $K_{\alpha 1}$ and $K_{\alpha 2}$ lines, of very similar wavelengths and which are, for this reason, not easily separable.

The frequency of the characteristic line corresponding to a given transition is related to the atomic number of the element that gave rise to it, $Z$, by Moseley's law

$$\nu = C(Z - \sigma)^2 \tag{4.3}$$

where the constant $C$ depends on the atomic energy levels involved in the transition and the constant $\sigma$ takes into account the interactions with other electrons. Thus, in a plot of $\nu^{1/2}$ as a function of $Z$ for a given transition the points corresponding to different target elements lie in a straight line and different lines are obtained for the $K_{\alpha_1}$, $K_{\alpha_2}$, $K_{\beta_1}$, etc., transitions. The characteristic frequency is higher the higher the atomic number and so the Mo $K_\alpha$ line ($Z = 42$) has a higher frequency and therefore a higher energy than the Cu $K_\alpha$ line ($Z = 29$). A full list of the wavelengths of the characteristic lines of the elements which are used in X-ray diffraction studies can be found in the *International tables for x-ray crystallography*.[1] Here, we will just point out that the two most frequently used lines are the Cu $K_\alpha$ line, $\lambda = 1.5418$ Å and the Mo $K_\alpha$ line, $\lambda = 0.7107$ Å. Both are doublets of slightly different wavelengths as pointed out before.

The intensity of a characteristic K line can be calculated using the equation:

$$I_K = Bi(V - V_K)^{1.5} \tag{4.4}$$

where $B$ is a constant, $i$ the electrical current, and $V_K$ the excitation potential of the K series, a quantity which is proportional to the energy required to remove a K electron from the target atom. It can be shown[2] that the ratio $I_K/I_W$ is a maximum if the accelerating potential is chosen to be $V = 4V_K$. If this condition is fulfilled, the $K_\alpha$ line is about 90 times more intense than the white radiation of equal wavelength ($I_W$). The $K_{\alpha_1}$ line is approximately twice as intense as the $K_{\alpha_2}$ line and the ratio $K_\alpha/K_\beta$ depends on $Z$ but it averages 5 (see Rieck[1]). The data collection methods that use monochromatic radiation discussed later all use $K_\alpha$ radiation and therefore require the elimination of the $K_\beta$ component of the spectrum which is always present. The methods used to achieve this are discussed on p. 241.

## Sealed-tube and rotating-anode generators

A conventional generator consists of a high-voltage power supply with electronic controls, connected to either a sealed tube or to the cathode of a

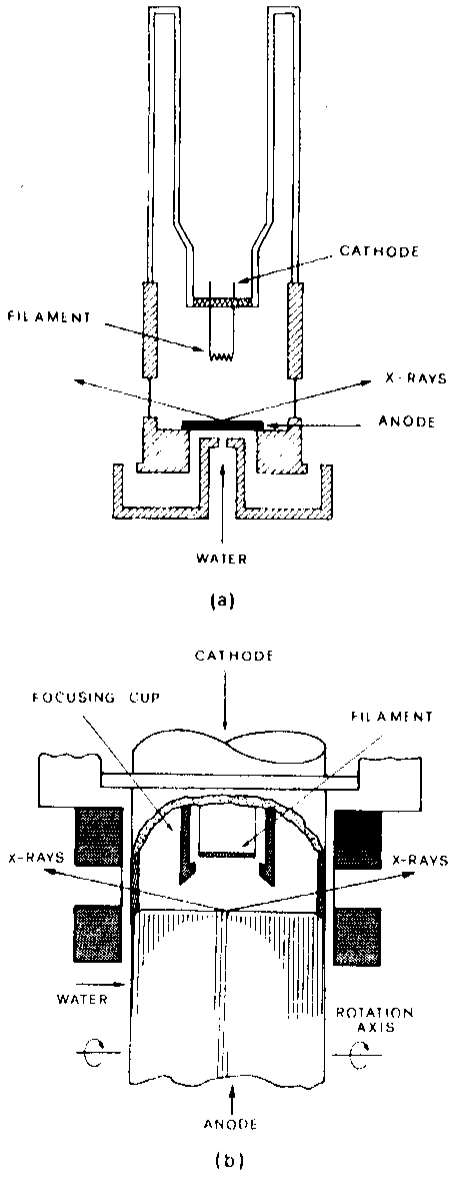


Fig. 4.3. (a) A sealed X-ray tube. (b) Sketch of a rotating-anode chamber. The path followed by the water that cools the anode is not shown in the figure. The anode is cylindrical and rotates about the axis shown.

rotating-anode generator. In the second case there must also be a way of making, keeping, and monitoring the high vacuum required for X-ray generation. Just how high the voltage to be applied must be, can be estimated from the considerations of the previous paragraphs and taking an excitation voltage given by Rieck.[1] This value for the copper K energy level is 8.981 kV so if one wishes to apply a voltage of 4 times $V_K$ about 36 kV have to be applied. For molybdenum even higher voltages are required.

The sketch of a sealed X-ray tube is shown in Fig. 4.3(a). It consists of a cathode with a filament that emits the electrons that are accelerated under vacuum by the high voltage applied and hit the fixed anode made of the metal whose characteristic spectrum has a $K_\alpha$ line of a wavelength which is adequate for the diffraction experiment to be performed. The high vacuum is necessary because the presence of gas molecules in the tube decreases the efficiency of the X-ray generating process by collisions with the electrons in the beam.

The process of X-ray production discussed in the previous section is highly inefficient: only about 0.1 per cent of the power applied is transformed into X-rays, the rest being dissipated as heat. In order to avoid melting of the target, it therefore becomes necessary to cool it, which is done by circulating cold water as shown in the figure. It is the efficiency of the cooling system that ultimately determines the maximum power that can be applied to the tube. The problem of heat dissipation also dictates the choice of the focal area of the beam of electrons on the anode. This area is always chosen to be rectangular with the sides in a ratio of at least six to one. In this way, when one looks at the focused electron beam on the target, which determines the surface that produces X-rays, in the direction of the longest side of the rectangle one can see, by choosing the appropriate angle, a small square focus with a side equal to the smallest rectangle side. At the same time, the real area that dissipates heat is several times that of a square of that size. The X-rays generated come out of the tube through four beryllium windows: the two that are shown in the figure, that are found in the direction of the longest axis of the rectangular focus, and another two in a direction perpendicular to it. The first two windows are used for single-crystal work, the others may be used when a linear focus is needed.

In rotating-anode generators, the target area seen by the electron beam is continuously renovated because the anode is rotated. In this way, much higher powers per unit of focal area can be applied to the unit and consequently higher X-ray intensities can be produced. Figure 4.3(b) is a sketch of a rotating anode chamber showing the two X-ray windows used for single-crystal work, the filament, placed with its longest axis parallel to the direction of the windows, the focusing cup, used to focus the electron beam on the target, and the anode which rotates about an axis parallel to the direction of the windows.

In a rotating-anode generator, the chamber has to be kept under vacuum for the reasons stated before, water has to be circulated to cool the anode as is done in the case of a sealed tube, and of course the anode has to be rotated at a certain speed. The system is therefore mechanically much more complicated than a tube and it requires a fairly frequent and demanding maintenance work. Figure 4.4 is a photograph of a modern rotating anode X-ray generator. Phillips[3] gives a detailed discussion of the advantages of

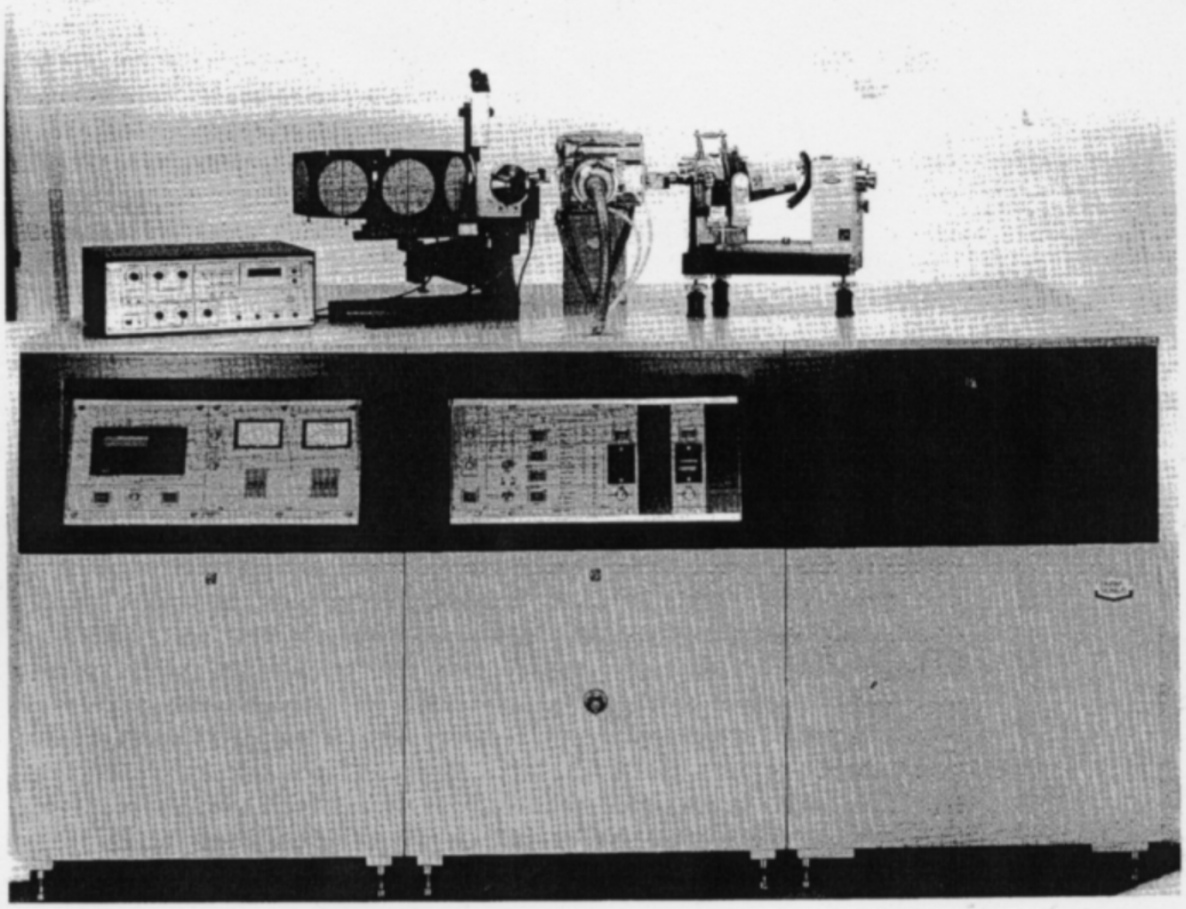

**Fig. 4.4.** A rotating-anode X-ray generator. (Photograph courtesy of Enraf Nonius.)

rotating-anode generators together with an exhaustive description of the practical problems encountered in their operation.

## Choice of the type of radiation

As discussed above, the $K_\alpha$ lines are those of highest intensity and therefore they are the ones that are normally used for standard X-ray diffraction work. Thus, in practice, the choice of the wavelength of the X-rays generated by conventional equipment is limited to the values of the characteristic $K_\alpha$ lines of the metals commonly used as targets. Two of these metals are most frequently used: copper and molybdenum; their $K_\alpha$ transitions generate radiation with a wavelength of about 1.5 and 0.7 Å respectively. As will be seen later, for a given crystal-to-detector distance and unit cell, the diffracted beams will be more separated on the detector if a longer wavelength is used. Thus, copper is used for macromolecular work in which one usually was large unit cell parameters and for the structure determination of organic molecules, which do not contain atoms that absorb this radiation strongly. Absorption of the radiation by the sample is therefore also a primary consideration in the selection of the wavelength to be used.

Another consideration is the maximum resolution of the reflections that will be recorded. We saw on p. 155 that there is a limiting sphere of radius

$2/\lambda$ that limits the volume of reciprocal space accessible to diffraction experiments. This sphere obviously has a different size for the two types of radiation discussed and therefore molybdenum radiation may be required to record data to a resolution not accessible to copper radiation.

Finally we mention the detection efficiency of the method that will be used to record the diffracted intensities. Film is a better detector for copper than for molybdenum radiation and some area detectors have been optimized for use with copper radiation. On the other hand, diffractometer counters have a very high counting efficiency for the Mo $K_\alpha$ radiation which explains why this type of radiation is so widely used for small-molecule single-crystal X-ray diffraction work.

## Synchrotron radiation

X-rays, as well as other types of electromagnetic radiation, can also be generated by sources known as synchrotron radiation facilities. In these installations either electrons or positrons are accelerated at relativistic velocities along orbits of very large radii, several metres or even hundreds of metres. These sources are, by necessity, very complex and those that produce suitable X-rays are limited, located mainly in the United States and Europe. However, since, as we will see, the X-rays they produce are in many ways much better than those generated by conventional sources, their use has grown steadily in the crystallographic community. As a result, more beam time has been made available to crystallographers and more synchrotron sources are planned for construction in different countries. Among those, the 6 GeV storage ring to be built in the USA[4] and the European Synchrotron Radiation Facility,[5] designed specifically to produce the best possible X-rays, promise to be of special importance is the development of this field.

From the extensive literature that exists in this ever expanding field we recommend two very elementary descriptions,[6,7] an introductory textbook,[8] and a more advanced treatise in several volumes.[9] In this last treatise chapters 1, 2, and 11 of volume 1 are specially relevant to our discussion; volume 3 of the series is totally devoted to X-ray methods.

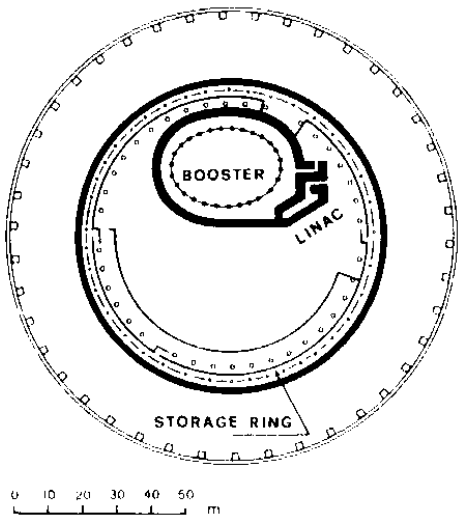


**Fig. 4.5.** Outline of a typical synchrotron radiation facility. The electrons or positrons are accelerated in the linear accelerator (linac) and then in the booster to be finally injected into the storage ring where they are kept circulating for periods of several hours. The beam lines, not shown in the figure, are tangential to the particle trajectory. Notice the scale at the bottom of the picture corresponding to 0–50 m.

## Generation of X-rays in a synchrotron radiation source

It is well known that charged particles moving under the influence of an accelerating field emit electromagnetic radiation. The energy of this radiation is dependent on the velocity of the particle. If the velocity is like that of the electrons moving in an antenna, emission takes place in the radio-frequency range but when the charged particles, electrons, or positrons, move with a speed approaching that of light, the spectrum extends into higher energy regions covering the X-ray range. An additional consequence of relativistic effects is a distortion of the angular distribution of the radiation. When the charged particles move at velocities approaching that of light, radiation is emitted in a very narrow cone parallel to the instantaneous velocity. In a synchrotron source the charged particles are made to move in closed trajectories, often circular or elliptical, and so the radiation is generated in cones tangent to the path followed by the particles (see for example chapter 1 of Koch[9]).

Figure 4.5 shows the essential elements of a synchrotron radiation source.

Notice the scale at the bottom which gives an idea of the size of this type of facility. The basic element of the installation from which radiation is generated is the storage ring, a toroidal cavity in which the charged particles are kept circulating under vacuum. An extremely high vacuum is required or else the particles are lost by collision with the atoms present in the cavity. Prior to injection into the storage ring, the particles must be accelerated, for example, first by a linear accelerator and then by a booster as shown in the figure. The other two elements that are essential to the operation of the ring are the so-called lattice, that is the set of magnets which force the particles to follow a closed trajectory as well as performing other functions, and the radio-frequency cavity system which restores to the particles the energy they lose as synchrotron radiation. The beam lines, not shown in the figure, are tangential to the storage ring.

It can be shown that a charged particle moving along a circular orbit emits as electromagnetic radiation the following power[8,9]

$$P = \frac{2e^2cE^4}{3R^2(m_0c^2)^4} = \frac{2e^2c\gamma^4}{3R^2} \tag{4.5}$$

where $P$ is the energy emitted per unit time, $e$ is the particle charge, $c$ the speed of light, $E$ the energy of the particle, $m_0$ its mass at rest, and $R$ the bending radius of the orbit. This equation explains why high-energy particles are required and also why only electrons or positrons are used. The power emitted by heavier particles such as protons is too low to be of significant importance.

The quantity $\gamma$, the ratio of the total energy to the rest energy of the particle, is of considerable importance since it is approximately related to the opening angle of the cone of radiation by

$$\Delta\psi \cong 1/\gamma \tag{4.6}$$

where $\Delta\psi$ is the emission angle in radians. A more exact relationship between these two parameters is given in reference [10].

The total power emitted by the ring is the power emitted by a particle in one revolution multiplied by the number of particles and divided by the time it takes them to complete a revolution.

The total power can be shown to be equal to[8,9]

$$P_{\text{tot}} = 26.6E^3Bi \tag{4.7}$$

where the energy of the particles is measured in GeV, the magnetic field $B$ in tesla, the current $i$ in amperes and the power is obtained in kW. The power is thus seen to be directly proportional to the current in the storage ring.

The radiation emitted at a modern storage ring comes from two sources: the bending magnets and the insertion devices. The first is the radiation we have discussed so far, the second is generated by special devices called wigglers and undulators which are briefly discussed below.

An important property of the radiation generated by bending magnets is its wide spectral distribution which can be described quantitatively in terms of the spectral flux $N$ which is the number of photons emitted per unit time interval into a relative band width $\Delta\lambda/\lambda$ into an angle element $d\theta$ in the plane of the electron orbit and integrated in the vertical plane. It can be shown that the flux of radiation normalized to the ring current generated by

bending magnets is equal to[8]

$$N(h\nu) = 1.256 \times 10^7 \, \gamma \, G_1(y) \text{ photons s}^{-1} \text{ mrad}^{-1} \text{ mA}^{-1}$$

(0.1% band width) (4.8)

where the factor $G_1(y)$ is an energy-dependent function that can be found tabulated for example in the book by Margaritondo.[8] The variable $y$ is defined as follows

$$y = h\nu/E_c$$

where $E_c$ is the critical energy associated with a magnetic field $B$ which in keV is given by

$$E_c = 2.22 \, E^3/R \tag{4.9}$$

where $E$ is measured in GeV and $R$, the radius of the bending magnet in metres. An alternative expression for $E_c$ is

$$E_c = 0.665 \, E^2 B \tag{4.10}$$

with $B$ measured in tesla.

A widely used parameter related to the critical photon energy is the critical wavelength $\lambda_c$

$$E_c = h\nu_c = hc/\lambda_c = 12.4/\lambda_c \tag{4.11}$$

where $E_c$ is measured in keV and $\lambda_c$ in Å.

The spectra of total emitted flux for several synchrotron radiation sources is shown in Fig. 4.6 taken from Materlik.[10] The critical wavelength, $\lambda_c$, is useful as an indicator of the suitability of a source for X-ray experiments. As can be seen in the figure although it does not correspond to the maximum flux it is close enough to give a good idea of the position of this maximum. It can be shown that ideally the wavelength used at a synchrotron source should fall in the range $0.25\lambda_c$ to $4.0\lambda_c$. Table 4.1, taken from the literature,[5] gives $E_c$, $\lambda_c$, and other relevant parameters for the

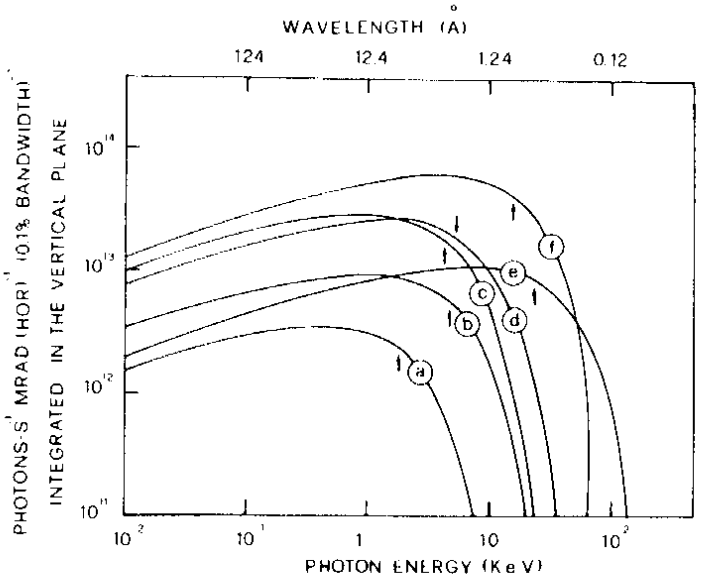


**Fig. 4.6.** Spectral distribution of several storage rings; a = ADONE (Frascati, Italy) (1.5 GeV, 105 mA); b = DCI (Orsay, France) (1.8 GeV, 250 mA); c = SRS (Daresbury, UK) (2.0 GeV, 685 mA); d = NSLS (Brookhaven, USA) (2.5 GeV, 500 mA); e = DORIS (Hamburg, Germany) (5.0 Gev, 100 mA); f = ESRF (Grenoble, France) (5.0 GeV, 565 mA). The critical wavelengths are indicated by arrows, notice their position relative to the maxima. Recall that the photon energy of the Cu $K_\alpha$ line corresponds to about 8 keV and that of the Mo $K_\alpha$ line to about 17 keV. HOR = horizontal plane. (Figure taken from Materlik.[10])

**Table 4.1.** Relevant parameters of the Synchrotron Radiation Sources in operation in 1987 (taken from reference 5)

| Name | Location | E(GeV) | R(m) | i(mA) | $E_c$(keV) | $\lambda_c$(Å) | Emittance ($\times 10^9$ m rad) | Insertion (devices) |
|---|---|---|---|---|---|---|---|---|
| Group I, $E_c \leq 0.06$ keV | | | | | | | | |
| N-100 | Karkhov, USSR | 0.10 | 0.5 | 50 | 0.004 | 3 100.0 | | |
| Surf II | Washington, USA | 0.25 | 0.84 | 25 | 0.041 | 302.4 | 27 | |
| Tantalus I | Wisconsin, USA | 0.24 | 0.64 | 200 | 0.048 | 258.3 | 27 | 2 |
| Group II, $E_c$ 0.06–2 keV | | | | | | | | |
| Sor ring | Tokyo, Japan | 0.4 | 1.1 | 250 | 0.13 | 95.4 | 30 | 1 |
| Siberia I | Moscow, USSR | 0.45 | | | | | | |
| Max | Lund, Sweden | 0.55 | 1.2 | 370 | 0.30 | 41.3 | 3 | 2 |
| COSY | Berlin, Germany | 0.56 | | | | | 250 | |
| Teras | Tsukuba, Japan | 0.6 | | | | | | |
| ACO | Orsay, France | 0.7 | 1.1 | 100 | 0.32 | 38.8 | 15 | 1 |
| NSLS | Brookhaven, USA | 0.75 | 1.9 | 500 | 0.4 | 31.0 | 13 | 2 |
| UV SOR | Okazaki, Japan | 0.75 | 2.2 | 500 | 0.43 | 28.8 | 8.10 | 2 |
| Fian C-60 | Moscow, USSR | 0.67 | 1.6 | 10 | 0.44 | 28.2 | | |
| Vepp-2M | Novosibirsk, USSR | 0.80 | 1.22 | 100 | 0.54 | 23.0 | | 2 |
| Hesyrl | Hefei, China | 0.8 | | | | | 9 | 3 |
| Superaco | Orsay, France | 0.8 | 1.75 | | | | 3.8 | 6 |
| SPRL | Stanford, USA | 1 | 2.1 | 500 | 1.05 | 11.8 | 2 | 5 |
| Bessy | Berlin, Germany | 0.8 | 1.83 | 500 | 0.62 | 20.0 | 4 | 1/2 |
| Aladdin | Wisconsin, USA | 1.3 | 2.08 | 500 | 1.07 | 11.6 | 6 | 3 |
| INS-ES | Tokyo, Japan | 1.3 | 4.0 | 30 | 1.22 | 10.2 | | |
| Pakhara | Moscow, USSR | 1.36 | 4.0 | 300 | 1.22 | 10.2 | | |
| Sirius | Tomsk, USSR | 1.36 | 4.23 | 15 | 1.32 | 9.4 | | |
| Adone | Frascati, Italy | 1.5 | 5.0 | 60 | 1.5 | 8.3 | 22.5 | 2–4 |
| Group III, $E_c$ 2–30 keV | | | | | | | | |
| DCI | Orsay, France | 1.8 | 4.0 | 300 | 3.63 | 3.4 | 1500 | 1 |
| SRS | Daresbury, UK | 2.0 | 5.55 | 500 | 3.2 | 3.9 | 150 | 1/4 |
| Vepp-3 | Novosibirsk, USSR | 2.25 | 6.15 | 100 | 4.2 | 3.0 | 150 | 2 |
| Photon Factory | Tsukuba, Japan | 2.5 | 8.33 | 500 | 4.16 | 3.0 | 50/15 | 2/7 |
| NSLS | Brookhaven, USA | 2.5 | 8.17 | 500 | 4.2 | 3.0 | 8 | 4/5 |
| Bonn | Bonn, Germany | 2.0 | 7.6 | 50 | 2.3 | 5.4 | | |
| Siberia II | Moscow, USSR | 2.5 | 5 | 300 | 6.9 | 1.8 | 8 | 3 |
| BEPC | Beijing, China | 2.8 | | | | | 66 | 8 |
| Elsa | Bonn, Germany | 3.5 | 10.1 | 50 | 9.3 | 1.3 | 50 | 1 |
| Arus | Erevan, USSR | 4.5 | 24.6 | 1.5 | 8.22 | 1.5 | | |
| Spear | Stanford, USA | 4.0 | 12.7 | 100 | 11.1 | 1.1 | 45 | 4/12 |
| Doris II | Hamburg, Germany | 5.0 | 12.1 | 50 | 22.9 | 0.5 | 570 | 1/7 |
| Tristan ACC | Tsukuba, Japan | 6/8 | | | | | 48 | 3 |
| Group IV, $E_c > 30$ keV | | | | | | | | |
| CESR | Ithaca, USA | 8.0 | 32.5 | 100 | 35.0 | 0.35 | 20 | 1/3 |
| Vepp-4 | Novosibirsk, USSR | 7.0 | 16.5 | 10 | 46.1 | 0.27 | | 2 |
| Petra | Hamburg, Germany | 18.0 | 192.0 | 18 | 67.4 | 0.18 | | |
| PEP | Stanford, USA | 18.0 | 165.5 | 10 | 78.0 | 0.16 | 15 | 1 |
| Tristan | Tsukuba, Japan | 30.0 | | | | | 18 | |

synchrotron sources in operation in 1987. If the spectral flux is transformed into power, i.e. the number of photons is multiplied by the energy of a photon $h\nu$, it can be shown that half the total power is irradiated below and half above the critical value $\lambda_c$.

Other parameters of interest are the source size and the divergence of the irradiated beam. The charged particle beam in the storage ring has a Gaussian profile characterized by the parameter $\sigma_x$, in the horizontal and $\sigma_z$ in the vertical plane. The full width at half maximum of the beam can then

be calculated as $2.35\sigma$ and the source area $F$ is estimated as

$$F = 2.35^2 \sigma_x \sigma_z.$$

Similarly the angular distribution is characterized by the parameters $\sigma_{x'}$ and $\sigma_{z'}$ and the solid angle of emission is then estimated as

$$\Omega = 2.35^2 \sigma_{x'} \sigma_{z'}.$$

Although $\sigma_x$, $\sigma_{x'}$ and $\sigma_z$, $\sigma_{z'}$ vary along the orbit their variations are correlated and it is thus useful to define another parameter, the emittance, which at special symmetry positions is found to be

$$\begin{aligned} \varepsilon_x &= \sigma_x \sigma_{x'} \\ \varepsilon_z &= \sigma_z \sigma_{z'}. \end{aligned} \tag{4.12}$$

The emittance is instead a constant along the charged particle path and it is thus another important parameter characteristic of an installation. The emittances of the synchrotron sources in operation in 1987 are also shown in Table 4.1.

Another useful function, which is often used to compare the potential performance of two sources, is the spectral brightness, also called spectral brilliance,[8] defined as the number of photons emitted per unit area of the source at point $x$, $z$ over a 0.1 per cent relative band width per unit solid angle $d\Omega$ and unit time in the direction defined by the angles $\psi$ (defined by the instantaneous velocity of the charged particle and the projection of the direction of observation onto the vertical plane) and $\theta$ (defined by the projection onto the horizontal plane instead). It can be shown that the spectral brightness $b$ is equal to (see Margaritondo[8] chapter 2)

$$b = N(2\pi)^{-3/2}(\sigma_x \sigma_z \sigma_\psi)^{-1} \exp[-(x/2\sigma_x)^2 - (z/2\sigma_z)^2 - (\psi/2\sigma_\psi)^2]$$

where $N$ is the spectral flux. If one defines the central brightness $b_c$ which is the brightness for $x = z = \psi = 0$ it is obvious that

$$b_c = N(2\pi)^{-3/2}(\sigma_x \sigma_z \sigma_\psi)^{-1}. \tag{4.13}$$

From this equation it can be seen that the brightness can be increased by increasing the flux or by decreasing the $\sigma$s. Decreasing the $\sigma$s can be accomplished by reducing the emittance of the storage ring (eqn (4.12)). The emittance of a ring is thus a fundamental parameter to be taken into account in comparing the expected performance from two different sources.

A radiation spectrum quite different from that produced by bending magnets can be obtained by the use of insertion devices. These are a series of periodically spaced magnets of alternating polarity which are inserted in a straight region of the ring and which do not alter the ideal closed orbit of the particles in the storage ring. Most insertion devices create a sinusoidal magnetic field which forces the charged particles to oscillate around the mean orbit. According to their characteristics they are called wigglers or undulators.

The parameter that has to be examined to determine whether an insertion device is a wiggler or an undulator is the $K$ parameter

$$K = \alpha\gamma = \frac{eB_0\lambda_0}{2\pi m_0 c} = 0.934 B_0 \lambda_0 \tag{4.14}$$

where $\alpha$ is the maximum deflection angle of the electron or positron trajectory, $B_0$ is the oscillating magnetic field measured in tesla and $\lambda_0$ is the period of the magnetic array measured in centimetres. Recalling that $1/\gamma$ is approximately equal to the natural opening angle $\Delta\psi$, $K$ becomes the ratio between the maximum deflection angle of the electron trajectory along the insertion device, $\alpha$, and $\Delta\psi$.

When the parameter $K \gg 1$ the device is called a wiggler. The effect of a wiggler on the emitted spectrum is to shift the critical energy $E_c$ to higher values and to increase the intensity of the radiation by a factor proportional to the number of periods of the magnetic array. No interference effects are observed and so the emitted spectrum is qualitatively very similar to that obtained from bending magnets.

If the parameter $K \ll 1$ the device is called an undulator and interference occurs between radiation which is emitted by the same electron at different points in its path through the device. As a result, radiation is emitted as a series of relatively sharp peaks whose wavelengths are given by the equation[10]

$$\lambda_i = \frac{\lambda_0}{2\gamma^2 j}\left(1 + \frac{\alpha^2\gamma^2}{2} + \gamma^2\theta^2\right) \tag{4.15}$$

where $\theta$ is the angle at which radiation is emitted and $j$ is the harmonic number. As is evident from this equation, the wavelength of the peaks can be shifted by changing the parameters that appear in parentheses, $\theta$ the angle of observation and $\alpha$ which, as we have seen, is related to the magnetic field of the device $B_0$. The intensity which is produced by an undulator with $N$ poles at $\theta = 0$ is amplified by a factor proportional to $N^2$.[10]

## Comparison of synchrotron and conventionally generated X-rays

We have seen on p. 233 that in practice only the characteristic lines of copper and molybdenum are sufficiently intense for use in crystallographic X-ray work and thus with conventional sources one is limited to only a discrete number of possible wavelengths. Synchrotron radiation does not have this limitation as should be clear from Fig. 4.6. The spectrum emitted is very wide and in fact extends in both directions far beyond the range spanned by the Cu $K_\alpha$ and Mo $K_\alpha$ lines. The possibility of selecting the wavelength for X-ray diffraction work has not been fully exploited although it is clear that it has far-reaching consequences. It can be used for example to solve the phase problem in macromolecular work (see Chapter 8, p. 544) by measuring anomalous dispersion effects (see for example Hendrikson *et al.*[11]). Furthermore, crystal absorption and radiation damage (see pp. 304 and 308) are wavelength dependent and thus can be minimized by optimixing the X-ray wavelength used.[12]

Probably the best known property of synchrotron radiation is its high brightness, resulting from the small cross-section of the charged particle beam and the high degree of collimation of the radiation.

A detailed comparison of the brightness and other properties of X-rays produced by synchrotron sources and sealed-tube and rotating-anode generators can be found in Bonse.[13] In Fig. 4.7, taken from Eisenberger,[4]

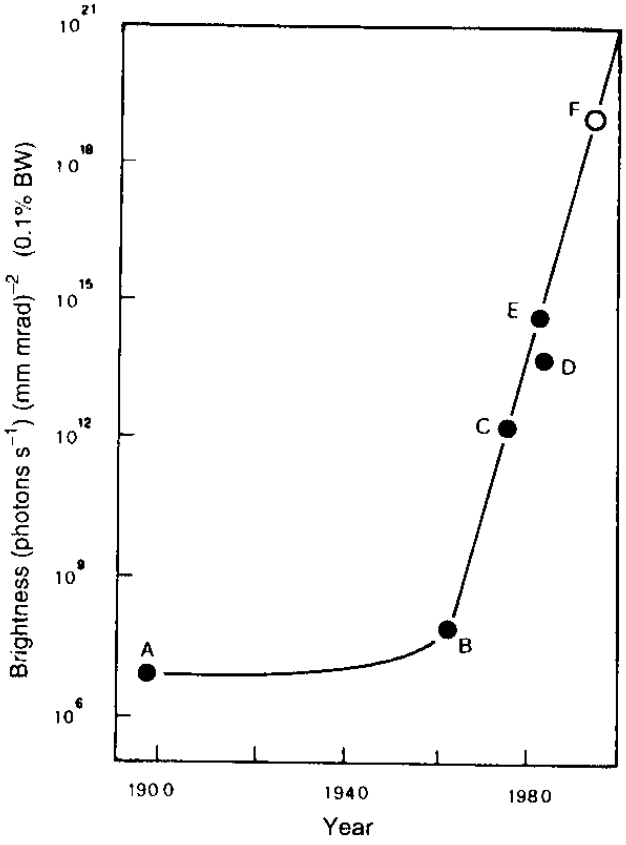


**Fig. 4.7.** The brightness of x-ray sources as a function of the year in which they became available. The points correspond to the following sources: A = X-ray tube; B = rotating-anode generator; C = Stanford Synchrotron Radiation Laboratory (SSRL) bending magnet; D = Brookhaven National Synchrotron Light Source (NSLS) bending magnet; E = SSRL 54 pole wiggler; F = 6 GeV source with undulator. (Figure taken from Eisenberger.[14])

the brightness of X-ray sources is plotted as a function of the year in which they became available. In the figure one can see that radiation from bending magnets, which, as we have seen, are the least intense of the possible synchrotron sources, can be $10^5$ times more intense than that from a rotating-anode generator. As a result, data collection at a synchrotron source is faster, produces higher-resolution data, and permits single-crystal work with specimens that can be only a few $\mu m^3$ in volume.[14] A sample of such a small size can only be treated as a polycrystalline material with a conventional source.

An important property of synchrotron radiation is that it is completely linearly polarized in the plane of the orbit of the charged particles and elliptically above and below this plane.[9] X-rays generated from conventional sources are totally non-polarized. As a result diffracted intensities have to be corrected for this polarization effect in different ways as we will see later (p. 303).

We mentioned before that the energy emitted by the moving charged particles is replenished by a radio-frequency cavity. Only the particles with an adequate phase relation with respect to the radio-frequency field can keep a stable orbit and they end up gathered in bunches which have a length that is dependent on the radio frequency used. The number of bunches of charged particles circulating around the orbit is an integer and can be regulated by varying the parameters of operation. Thus, synchrotron radiation is, in fact, produced at a given point in the orbit as a flash when a bunch passes through that point. As a result, synchrotron radiation has a well defined time structure, that is, pulses of radiation are emitted at

perfectly defined time intervals. For example the European Synchrotron Radiation Facility is planned to produce pulses lasting from 65 to 140 ps and the pulses will be separated by a minimum of 3 ns.[15] This property of synchrotron radiation, of clear importance in time-resolved studies, has received so far very little attention in X-ray diffraction work.

## Monochromatization, collimation, and focusing of X-rays

We have seen that conventional X-ray sources generate the discrete lines of the characteristic spectrum of the anode superimposed on the white radiation continuum and that radiation is emitted in every possible direction, and that although synchrotron sources emit a spatially confined narrow beam, the wavelength of this radiation spans a very wide continuous spectrum. All of the data collection methods discussed later require that a narrow pencil of X-rays strike the specimen under examination and, in addition, most of them also require that the energy of the radiation be limited to a wavelength band as narrow as possible. Ideally the radiation should consist of photons of only a single wavelength. Here we discuss the methods used to select a narrow wavelength out of the spectrum generated by the source and how to define a narrow parallel beam of X-rays to be used for diffraction experiments in conjunction with the data collection devices discussed later.

### Filters

One way to select a wavelength interval out of the spectrum generated by the source is by filtering the radiation through a material that selectively absorbs the unwanted radiation while letting through most of the photons of the wavelength that will be used for the diffraction experiment. The absorption of X-rays by a material follows Beer's law:

$$I/I_0 = e^{-\mu x} \tag{4.16}$$

where $I$ is the transmitted intensity, $I_0$ the incident intensity, $x$ the distance travelled by the X-rays in the material, i.e. the thickness of the filter, and $\mu$ is the linear absorption coefficient which depends on the substance, its density, and the wavelength of the X-rays. Since $\mu$ depends on the density of the material, the quantity that is usually tabulated is $\mu_m = \mu/\rho$, the mass absorption coefficient, a characteristic of the substance that depends only on the wavelength considered. Complete tables of $\mu_m$ as a function of the wavelength for different materials used as filters can be found in Koch and MacGillavry,[15] and a plot of $\mu_m$ versus $\lambda$ for nickel is shown in Fig. 4.8 along with the radiation spectrum generated by a copper anode. In the figure it can be seen that the curve of $\mu_m$ versus $\lambda$ shows two continuous branches separated by a sharp discontinuity, called the absorption edge. If the filter is a pure element, the continuous parts of the curve follow approximately the equation

$$\mu_m = kZ^3\lambda^3 \tag{4.17}$$

where $k$ is a constant with different values for the two branches of the curve and $Z$ is the atomic number of the element. This equation shows why harder X-rays, i.e. X-rays with a shorter wavelength, are absorbed less than those

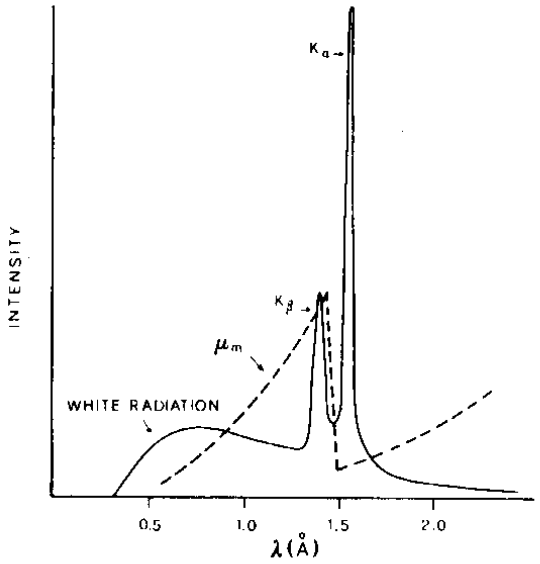


**Fig. 4.8.** The broken line represents the variation of the mass absorption coefficient $\mu_m$ as a function of the wavelength for nickel. The continuous line is the X-ray spectrum generated by a copper anode. Notice that the absorption edge of nickel falls in between the $K_\alpha$ and the $K_\beta$ characteristic lines of copper.

with a longer wavelength. The presence of the absorption edge in the curve is explained by the fact that the photons at the edge have the wavelength corresponding to the energy necessary to eject an electron from the K orbital of the atoms of the filter. Thus, when this energy is reached massive absorption of radiation occurs with photoionization of the filter and production of fluorescent radiation.

Similarly to the displacement of the position of the characteristic lines with $Z$, absorption edges move to shorter wavelength as the atomic number of the element increases. A common single filter is chosen so that its absorption edge falls in between the $K_\alpha$ and the $K_\beta$ peaks of the anode that has been used to generate the X-rays. In this way, the unwanted radiation of highest intensity, i.e. the unavoidable $K_\beta$ peak, can be greatly attenuated without reducing too much the intensity of the $K_\alpha$ peak that will be used for the experiment. Figure 4.8 shows that a nickel filter has its absorption edge at the wavelength necessary to very strongly absorb the copper $K_\beta$ peak. Since copper has $Z = 29$ and nickel $Z = 28$ there is a difference of one between the atomic numbers of the target anode used to generate the X-rays and the filter with an absorption edge falling in between its $K_\alpha$ and $K_\beta$ peaks. This is generally true for every element with $Z \leq 70$ and for the elements of the second long row of the periodic table it is also true that both the elements of $Z - 1$ and $Z - 2$ can be used to absorb the $K_\beta$ peak of the anode with atomic number $Z$. Thus both Nb ($Z = 41$) and Zr ($Z = 40$) can be used as filters for Mo ($Z = 42$) radiation.

The relative intensities of the $K_\alpha$ and the $K_\beta$ peaks depend not only on the absorption coefficient of the filter but also on its thickness. Roberts and Parrish[16] give a table of the appropriate filter thicknesses necessary to produce $K_\alpha/K_\beta$ ratios of 100 and 500 for different elements used as targets and filters. The same table gives also the percentage of $K_\alpha$ peak lost by filtering which can vary between about 40 and 70 per cent.

A variation of the simple filter technique is the Ross balanced-filter method.[16] In this method two filters are used: one with its absorption edge at slightly shorter and the other at slightly longer wavelength than the $K_\alpha$

peak selected. The thickness of the filters is chosen so that the radiation is absorbed to the same extent except in the interval in between the two absorption edges. With this technique two measurements are made with either one of the two filters in position and the measured intensity is then taken to be the difference between the two values obtained.

## Crystal monochromators

An alternative and more selective way to produce a beam of X-rays with a narrow wavelength distribution is by using a single-crystal monochromator.

Bragg's equation (3.32) shows that when radiation of different wavelengths impinges upon a crystal, diffracted beams are observed at scattering angles $\theta$ that depend on the wavelength of the radiation $\lambda$. Thus, selecting a given diffraction angle $\theta$ is equivalent to choosing a particular wavelength out of the spectrum incident on the crystal.

The simplest type of crystal monochromator consists of a single crystal with one face parallel to a major set of crystal planes mounted so that its orientation with respect to the X-ray beam can be properly adjusted. The most important properties of a crystal monochromator are:

(1) the crystal used must be mechanically strong and should be stable in the X-ray beam;

(2) the interplanar distance should be in the appropriate range to allow the selection of the desired wavelength at a reasonable scattering angle;

(3) the presence of one or more strong diffracted intensities that can be chosen so that the intensity loss of the beam, which is always appreciable, may be reduced as much as possible; and

(4) the mosaicity of the crystal, which determines the divergence of the diffracted beam and the resolution of the crystal, should be small.[17,18]

The reflection chosen should also have a scattering angle as small as possible in order to minimize the loss of intensity due to the polarization factor (see p. 303). Roberts and Parrish[16] give a table with the important properties of crystals commonly used as monochromators.

In a variation of this simple type of flat monochromator, the crystal surface is cut so that it forms an angle with the set of planes that diffract the radiation. In this way, the diffracted beam has a smaller width and as a result more photons are concentrated in a smaller cross section of the beam.[16] By properly curving their surface, crystal monochromators can be used to focus the X-ray beam in a very small area.[19] The curvature of the surface can be produced by simply bending the crystal, in which case the diffracting planes should ideally be tangential to the curved surface. If the monochromator is bent in the shape of a cylinder of elliptical section with the source in one of the foci, the reflected radiation will concentrate on the other focus of the ellipse. A further variation consists of not only bending the crystal but also in grinding its surface so that the radius of curvature of the diffracting planes of the crystal is different from that of its surface. The advantage of this type of monochromator is that it does not suffer from some optical aberrations present in singly bent crystals.[16] Curved crystal monochromators are frequently used to select the wavelength of synchrotron radiation. In addition to the requirements stated before, the

crystals should have in this case a very small thermal expansion and a large thermal conductivity because the power applied is much larger than in the case of conventional sources.[18]

Another type of monochromator of wide application in synchrotron sources is the double-crystal monochromator in which the incident X-ray beam is diffracted twice by two similar crystals. This type of monochromator can be constructed with different geometries designed to improve the resolution and/or to keep the X-ray beam in the original direction. A discussion of this type of crystal monochromator can be found in Margaritondo.[18] Crystal monochromators are more selective than filters and, in the case of conventional generators, are capable of resolving the $K_{\alpha_1}$ and $K_{\alpha_2}$ doublet which cannot be separated by any filtering method.

## Collimators

The function of collimators is to define a narrow cylindrical beam of X-rays that ideally should be as parallel as possible.

A simple pinhole collimator is shown sketched in Fig. 4.9. It consists of a cylinder with two apertures defining the beam and a third guard aperture which does not affect the beam size defined by the other two but eliminates the radiation scattered by the defining aperture furthest from the X-ray source. These apertures are commonly circular, although slits can be used instead in which case square or rectangular beams can be defined. Cylindrical beam pinhole collimators are typically used with conventional sources to define a beam of radiation that is monochromatized by either a filter or a crystal monochromator. Such collimators never produce an ideally parallel X-ray beam but, in addition to the parallel X-rays, they also produce convergent and divergent X-rays as shown in the figure. A conventional X-ray source, when viewed at the appropriate take-off angle is seen as a square. If $l$ is the distance between the two defining apertures $S_1$ and $S_2$ and $d$ is the diameter of the collimator the maximum angle of divergence of the beam, $\gamma$, can be calculated as shown in the figure as

$$\tan \gamma/2 = \frac{d/2}{l/2} = d/l$$

and since the angle is very small

$$\tan \gamma/2 \sim \sin \gamma/2 \simeq \gamma/2 = d/l \qquad \gamma = 2(d/l)$$

where $\gamma$ is calculated in radians.

If we substitute in this equation $d$ and $l$ for two reasonable values: 50 and 0.5 mm we can get an estimate for the maximum divergence $\gamma$

$$\gamma = 2 \times 0.5/50 = 2 \times 10^{-2} \text{ radians.}$$

Huxley[20] and more recently Arndt and Sweet[17] have extensively discussed the conditions that can be varied in order to optimize collimation. The

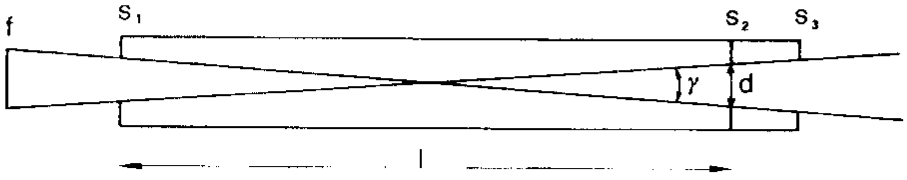


Fig. 4.9. Pinhole collimator showing the angle of greatest divergence $\gamma$, $S_1$ and $S_2$ are the two apertures defining the beam which are separated by the distance $l$, and have a diameter of $d$; $S_3$ is the guard aperture.

variables that can be adjusted are the crystal and X-ray focus size, the crystal to focus distance, and the crystal to detector distance. Depending also on the reflection to reflection resolution necessary for the experiment, different conditions are found which maximize the signal to noise ratio given the restrictions imposed by the experiment.

## Mirrors

X-rays can be reflected by mirrors when the angle of incidence is smaller than a certain critical angle $\theta_c$ which is a function of the wavelength $\lambda$ and can be calculated by the equation[17,19]

$$\theta_c = 2.32 \times 10^5 \left(\frac{Z\rho}{A}\right)^{1/2} \lambda \tag{4.18}$$

where $Z$ is the atomic number, $\rho$ the density, and $A$ the atomic weight of the reflecting material. If the angle of incidence is chosen to be within ten per cent of $\theta_c$ for the Cu $K_\alpha$ radiation, the X-rays having a wavelength shorter than the corresponding $\lambda$, in particular the fairly intense $K_\beta$ peak, will not be reflected and therefore they will be eliminated from the beam. Thus, by properly choosing the glancing angle of the X-rays on the mirror the radiation can be partially monochromatized. The values of the critical angles $\theta_c$ depend on the reflecting material as shown by the equation given above and they are, in general, very small: 14′ for glass and 23′ for nickel mirrors, calculated for a wavelength corresponding to the Cu $K_\alpha$ radiation. A table of this property and other parameters of interest of mirrors can be found in Witz.[19]

If the reflecting surface of the mirror is curved, ideally in the shape of an elliptical cylinder with the source in one focus, the reflected radiation will converge to the other focus of the ellipse and a very intense X-ray beam will be obtained at that point.

This principle is used in the design of a very powerful device that is used to focus and partially monochromatize an X-ray beam and which uses two curved mirrors with perpendicular axes of curvature.[21] This double-mirror system has been used for X-ray diffraction work on virus crystals which, having very large unit cell parameters, pose particularly serious problems for the spatial separation of the very close diffracted beams.[22] Mirrors are also very extensively used in the beamlines of synchrotrons. In addition to focusing and partial monochromatization they perform several other functions: splitting of a beam into two, magnification or demagnification of the source, and change in the polarization of the radiation.[18] The function to be performed determines their geometry and so their surface can be flat or curved and the mirror can be bent or segmented, that is constituted by several small flat pieces which are easier to produce than large curved single mirrors.

**Table 5.1** Relevant parameters of some synchrotron radiation sources in operation in 2001 having $E_c > 2$ keV

| Name | Location | $E$ (GeV) | $R$ (m) | Web source of information |
|---|---|---|---|---|
| APS | Argonne, IL, USA | 7.0 | 175.8 | http://www.aps.anl.gov/aps.php |
| BEPC | Beijing, China | 1.5–2.8 | 38.3 | http://www.ihep.ac.cn/bsrf/main.html |
| BESSY II | Berlin, Germany | 1.7 | 38.2 | http://www.bessy.de/BII/ |
| Boomerang* | Australia | 3.0 | 26.1 | http://www.ansto.gov.au/natfac/boomerang.html |
| CANDLE* | Yerevan, Armenia | 3.2 | 34.4 | http://www.candle.am |
| CHESS | Ithaca, NY, USA | 4.7–5.6 | 122.3 | http://www.chess.cornell.edu |
| CLS* | Saskatoon, Canada | 2.5–2.9 | 27.2 | http://www.cls.usask.ca |
| DORIS III | Hamburg, Germany | 4.5–5.3 | 46.1 | http://www-hasylab.desy.de |
| DIAMOND* | Didcot, UK | 3.0 | 55.7 | http://www.diamond.ac.uk |
| ELETTRA | Trieste, Italy | 2.0 | 41.2 | http://elettra.trieste.it |
| ESRF | Grenoble, France | 6.1 | 134.5 | http://www.esrf.fr |
| INDUS-2* | Indore, India | 2.0 | 27.4 | http://www.ee.ualberta.ca/~naik/cataccel.html |
| LNLS | Campinas, Brasil | 1.4 | 14.9 | http://www.lnls.br |
| LURE | Orsay, France | 1.8 | 15.0 | http://www.lure.u-psud.fr |
| NSLS | Upton, NY, USA | 2.6–2.8 | 27.1 | http://nslsweb.nsls.bnl.gov/nsls |
| PF | Tsukuba, Japan | 2.5 | 29.8 | http://pfwww.kek.jp |
| PLS | Pohang, Korea | 2.0 | 44.6 | http://pal.postech.ac.kr |
| SESAME* | Allaan, Jordan | 1.0 | 15.9 | http://www.sesame.org.jo |
| SLS | Villigen, Switzerland | 2.4 | 45.9 | http://www.psi.ch/sls |
| SOLEIL* | Orsay, France | 2.5 | 47.8 | http://www.soleil.u-psud.fr |
| Spring-8 | Hyogo, Japan | 8.0 | 228.7 | http://www.spring8.or.jp |
| SRRC | Hsinchu, Taiwan | 1.5 | 19.1 | http://www.ssrc.gov.tw |
| SRS | Daresbury, UK | 2.0 | 15.3 | http://www.srs.ac.uk/srs |
| SSRL | Stanford, CA, USA | 3.0 | 8.4 | http://www-ssrl.slac.stanford.edu |

*These facilities are planned or in construction.

**Table 5.2** Comparison of the principal characteristics of conventionally- and synchrotron-generated X-rays. Conventional laboratory sources include sealed X-ray tubes, rotating anodes, and microsources

| X-ray source | Laboratory source | Synchrotron source |
|---|---|---|
| Photon flux at the sample (photons $s^{-1} mm^{-2} mrad^{-2}$ 0.1% bandwidth) | $10^7$–$10^9$ | $10^{13}$–$10^{23}$ |
| Natural divergence of the emitted radiation | Wide (in all directions) | 0.2–0.5 mrad (in the direction tangent to the electron orbit) |
| Energy range | Usable intensity only at characteristic wavelengths (depends on the anode material) | High-intensity tunable in a wide range around $\lambda_c$ |
| Time stability of the incident beam | Stable with time | Decays with time (incident beam normalization or fixed count accumulation are needed) |
| Polarization | Unpolarized | Totally polarized in the plane of the electron orbit |
| Time structure | None | Pulsed in the nanosecond range |
| Accessibility/cost | Available at little cost in most crystallographic laboratories | Available only at national or international large-scale facilities |